Nonlinear reference tracking control of a gas turbine with load torque estimation

B. Pongrácz [1,2], P. Ailer [3], K.M. Hangos, [1] and G. Szederkényi [1,*]

[1] *Process Control Research Group, Systems and Control Laboratory,*

Computer and Automation Research Institute, Hungarian Academy of Sciences, H-1518 Budapest, P.O.Box 63., HUNGARY

[2] *Dept. of Computer Science, Pannon University, H-8200 Veszprém, Egyetem u. 10., HUNGARY*

[3] *Knorr-Bremse Research and Development Ltd., H-1119 Major u. 69, Budapest, HUNGARY*

e-mail: pongracz@scl.sztaki.hu, Piroska.Ailer@knorr-bremse.com, hangos@scl.sztaki.hu, szeder@scl.sztaki.hu

SUMMARY

Input-output linearization based adaptive reference tracking control of a low power gas turbine model is presented in this paper. The gas turbine is described by a third order nonlinear input-affine state-space model, where the manipulable input is the fuel mass flowrate and the controlled output is the rotational speed. The stability of the one-dimensional zero dynamics of the controlled plant is investigated via phase diagrams. The input-output linearizing feedback is extended with a load torque estimator algorithm resulting in an adaptive feedback scheme. The tuning of controller parameters is performed considering three main design goals: appropriate settling time, robustness against environmental disturbances and model parameter uncertainties, and avoiding the saturation of the actuator. Simulations show that the the closed loop system is robust with respect to the variations in uncertain model and environmental parameters and its performance satisfies the defined requirements.

*Correspondence to: Computer and Automation Research Institute, Hungarian Academy of Sciences, H-1518 Budapest, P.O.Box 63., HUNGARY. Tel:+36 1 279 6000 +36 Fax: +36 1 466 7503, e-mail: szeder@scl.sztaki.hu

John Wiley & Sons, Ltd.

KEY WORDS: input-output linearization; adaptive control; reference tracking; gas turbine

1. INTRODUCTION

Gas turbines are important and widely used prime movers in transportation systems. Besides this main application area, gas turbines are found in power systems where they are the main power generators [1]. Therefore the modelling and control of gas turbines is of signficant practical importance.

Control techniques applied for gas turbines are most often based on linear controllers. These are mainly variants of PID controllers such as in [18] or state-space based linear controllers, e.g. an LQ-servo controller in [2]. Linear quadratic Gaussian control with loop transfer recovery (LQG/LTR) [3] and robust control system design have also been performed for gas turbines [4].

Nonlinear control approaches for gas turbine control include model predictive control [17, 19] or soft computing methods such as neural networks, genetic algorithms [16] and fuzzy controllers [14]. In [5], mathematical programming is proposed for optimal turbine control. However, none of the above mentioned studies examine the robustness of the proposed controllers with respect to the changing environmental conditions and uncertain physical model parameters. The application of classical nonlinear state-space methods in turbine control is not frequent, although several nonlinear control solutions seem to be promising from other application areas. For example, nonlinear adaptive control schemes can be applied to physically similar models in transportation engineering (see e.g. the nonlinear adaptive tracking control of an induction motor with uncertain load torque [6] or a robust backstepping-based control method with actuator failure compensation, applied to a nonlinear aircraft

model [7]).

In order to apply nonlinear state-space model based control, one has to develop a relatively simple (i.e. low dimensional) yet powerful model that is able to describe the nonlinear dynamic behaviour of the gas turbine. A strongly nonlinear third order state space description of a low power gas turbine of type DEUTZ T216 has been developed and identified from measured data [8], and its input-output linearization based regulation is presented in [9]. The main possibly time-varying disturbance during the operation of gas turbines is the load torque. In the case of turbines, similarly to other rotating machines like induction motors [21] or diesel engines [20], the value of the load torque gives very important state and diagnostic information about the system. Moreover, the knowledge of load torque can largely contribute to the design of more efficient control schemes [20]. However, the instrumental measurement of load torque is not always possible in practice, therefore dynamic model-based identification and estimation methods are often required to solve this problem.

It is well-known that exact and input-output linearization based control techniques are particularly sensitive to model parameter uncertainties [10] and require almost perfect matching between the real and the mathematical model to show the required performance. However, the following facts justify the choice of linearization over other possible nonlinear design methods. Firstly, the availability of a high fidelity nonlinear state-space model that was identified and validated from real measurement data. Secondly, linearization with the given input-output structure introduces the rotational speed and its time-derivative as state variables after the necessary coordinates transformation and this is advantageous and useful from a physical and engineering point of view. Thirdly, the linearization-based controller can serve as a basis for other nonlinear design schemes where the model or parameter uncertainties are further handled using an appropriate technique.

The outline of the paper is as follows. In section 2, a third order nonlinear state space model is

described briefly for the turbine. Section 3 deals with the stability of the zero dynamics with respect to the rotational speed, since it plays a key role in controller design. In section 4, a linear quadratic controller with load torque estimation is designed for the input-output linearized model. Finally, the simulation results and the most important conclusions are shown in sections 5 and 6, respectively.

2. DYNAMIC MODEL OF THE GAS TURBINE

The main parts of a gas turbine include the inlet duct, the compressor, the combustion chamber, the turbine and the nozzle or the gas-deflector. The operation principle of gas turbines is roughly the following. Air is drawn into the engine through the inlet duct by the compressor, which compresses it and then delivers it to the combustion chamber. Within the combustion chamber, the air is mixed with fuel and the mixture is ignited, producing a rise in temperature and hence an expansion of the gases. These gases are exhausted through the engine nozzle or the engine gas-deflector, but first they pass through the turbine, which is designed to extract sufficient energy from them to keep the compressor rotating, so that the engine is self sustaining. The main parts of a gas turbine are shown schematically in Fig. 1.

A real low-power gas turbine is used for our studies. The equipment is installed in the Budapest University of Technology and Economics, Department of Aircraft and Ships on a test-stand.

2.1. Dynamic model equations

The nonlinear state equations are derived from first engineering principles. Dynamic conservation balance equations are constructed for the overall gas mass m, its internal energy U and the mechanical energy E_{shaft} [11].

These dynamic equations have to be transformed into intensive variable form to contain the

measurable quantities. The set of transformed differential balances include the dynamic mass balance for the combustion chamber, the pressure form of the state equation derived from the internal energy balance for the combustion chamber and the intensive form of the overall mechanical energy balance expressed for the rotational speed n. This way, three independent balance equations can be constructed as state equations.

In order to complete the model, constitutive algebraic equations are also needed. These equations describe the static behaviour of the gas turbine in various operating points, and all of them can be substituted into the dynamic equations [11].

The final form of the nonlinear dynamic model equations is the following:

$$\frac{dm_{Comb}}{dt} = \nu_C + \nu_{fuel} - \nu_T \tag{1}$$

$$\frac{dp_3^{tot}}{dt} = \frac{R}{V_{Comb}c_v}\left(\nu_C c_p T_1^{tot}\left(1+\frac{1}{\eta_C}\left(\left(\frac{p_3^{tot}}{p_1^{tot}\sigma_{Comb}}\right)^{\frac{\kappa-1}{\kappa}}-1\right)\right) - \nu_T c_p \frac{p_3^{tot}V_{Comb}}{m_{Comb}R} + Q_f \eta_{comb}\nu_{fuel}\right) \tag{2}$$

$$\frac{dn}{dt} = \frac{1}{4\Pi^2\Theta n}\left(\nu_T c_p \frac{p_3^{tot}V_{Comb}}{m_{Comb}R}\eta_T\eta_{mech}\left(1-\left(\frac{p_1^{tot}}{p_3^{tot}\sigma_I\sigma_N}\right)^{\frac{\kappa-1}{\kappa}}\right) - \nu_C c_p \frac{T_1^{tot}}{\eta_C}\left(\left(\frac{p_3^{tot}}{p_1^{tot}\sigma_{Comb}}\right)^{\frac{\kappa-1}{\kappa}}-1\right) - \frac{3M_{load}}{2\cdot 50\Pi\Theta}\right) \tag{3}$$

where

$$\nu_C = \beta\, A_1\, \frac{p_1^{tot}}{\sqrt{T_1^{tot}}}\left(a_1 \frac{n}{\sqrt{\frac{T_1^{tot}}{288.15}}}\frac{p_3^{tot}}{p_1^{tot}\sigma_{Comb}} + a_2\frac{n}{\sqrt{\frac{T_1^{tot}}{288.15}}} + a_3\frac{p_3^{tot}}{p_1^{tot}\sigma_{Comb}} + a_4\right) \tag{4}$$

$$\nu_T = \beta\, A_3\, \frac{p_3^{tot}}{\sqrt{\frac{p_3^{tot}V_{Comb}}{m_{Comb}R}}}\left(b_1 \frac{\tau\, n}{\sqrt{\frac{p_3^{tot}V_{Comb}}{m_{Comb}R}}}\frac{p_3^{tot}\sigma_I\sigma_N}{p_1^{tot}} + +b_2\frac{\tau\, n}{\sqrt{\frac{p_3^{tot}V_{Comb}}{m_{Comb}R}}} + b_3\frac{p_3^{tot}\sigma_I\sigma_N}{p_1^{tot}} + b_4\right) \tag{5}$$

The parameters, constants of the nonlinear dynamic model are previously known or determined from measurements. The detailed identification and validation procedure is described in [11]. The parameter values of the model can be found in Table II in the Appendix.

2.2. Nonlinear input affine state space model

The dynamic equations (1)-(3) can be transformed into the following standard input-affine form [10]:

$$\frac{dx}{dt} = f(x) + g(x)u \tag{6}$$

$$y = h(x) \tag{7}$$

with the state vector

$$x = [\, x_1 \;\; x_2 \;\; x_3 \,]^T = [\, m_{Comb} \;\; p_3^{tot} \;\; n \,]^T \tag{8}$$

and the only input variable

$$u = v_{fuel}. \tag{9}$$

The set of possible disturbances is the following:

$$d = [\, d_1 \;\; d_2 \;\; d_3 \,]^T = [\, p_1^{tot} \;\; T_1^{tot} \;\; M_{load} \,]^T \tag{10}$$

Finally, the f, g and h functions can be written as:

$$f(x) = \begin{bmatrix} f_1(x_1,x_2,x_3,d_1,d_2) \\ f_2(x_1,x_2,x_3,d_1,d_2) \\ f_3(x_1,x_2,x_3,d_1,d_2,d_3) \end{bmatrix}, \quad g(x) = \begin{bmatrix} c_1 \\ c_2 \\ 0 \end{bmatrix}, \quad h(x) = \begin{bmatrix} h_1(x_1,x_2,x_3,d_1) \\ x_2 \\ x_3 \end{bmatrix} \tag{11}$$

where c_1 and c_2 are constants. It is important to note that these functions do not only depend on the state variables, but also on the disturbance vector. Moreover, the elements of g are constants which means that the input enters the model equations linearly. The state, input, output and environmental disturbance variables are explained in Table I, while a comprehensive list is given in the Nomenclature.

The dynamical model of the gas turbine is valid within the following operating domain:

$$0.00305 \text{ kg} = x_{1min} \leq \quad x_1 \quad \leq x_{1max} = 0.00835 \text{ kg}$$

$$154837 \text{ Pa} = x_{2min} \leq \quad x_2 \quad \leq x_{2max} = 325637 \text{ Pa}$$

$$650 \, \frac{1}{s} = x_{3min} \leq \quad x_3 \quad \leq x_{3max} = 833.33 \, \frac{1}{s}$$

From now, this domain is denoted by $\mathscr{X}$. The structure of f and g is such that for every constant reference control input value there is a unique steady state point in $\mathscr{X}$.

3. ZERO DYNAMICS ANALYSIS

Roughly speaking, the zero dynamics (or zero output constrained dynamics) of a system gives us information about its internal behaviour, when the output is forced to be identically zero (or constant) [10]. Before the design of a linearization-based controller, it is essential to analyse the properties of the zero dynamics to be able to ensure the stability of the whole closed- loop system. In our case, the controlled output is the rotational speed, therefore the zero dynamics analysis is performed with respect to this output variable:

$$y_{ZD} = h_{ZD}(x) = x_3$$

using the nominal values of the disturbance variables. Let us denote the (piecewise constant) value of the rotational speed to be tracked by x_3^*.

As it can be seen from (11), the relative degree of our model is uniformly 2 in the operating region, since

$$L_g h_{ZD}(x) = \frac{\partial h_{ZD}}{\partial x} g(x) = 0, \quad x \in \mathscr{X}$$

and

$$L_g L_f h_{ZD}(x) \neq 0, \quad x \in \mathscr{X}$$

This means that the first and second derivative of the output can be written as

$$\dot{y}_{ZD} = L_f h_{ZD}(x) \tag{12}$$

$$\ddot{y}_{ZD} = L_f^2 h_{ZD}(x) + L_g L_f h_{ZD}(x) u \tag{13}$$

Using the constraints $y_{ZD} = x_3^*$ and $\dot{y}_{ZD} = 0$, we can write the one-dimensional zero dynamics as a function of x_2, i.e.

$$\dot{x}_2 = \phi(x_2)$$

The Lie-derivatives of h_{ZD} and the function ϕ are not given here in detail because of their complexity. Although ϕ is a function of only one variable, it is hard to analytically treat the sign of it. Thus, we apply a simple graphical method to examine the stability of the zero dynamics. Fig. 2 shows the phase diagrams of the zero dynamics belonging to four different constant values of the rotational speed. In all cases, the equilibrium point x_2^* (the point where the curve crosses the horizontal axis) is unique and stable in the operating domain of the turbine.

Although Fig. 2 illustrates zero dynamics with the nominal load torque only ($M_{load} = 50\ Nm$), phase diagrams of zero dynamics with a large number of investigated load torque values (between 0 Nm and 150 Nm) show that the operating points are unique and asymptotically stable in the whole operating domain $\mathscr{X}$ for arbitrary u^* in all cases.

4. INPUT-OUTPUT LINEARIZATION BASED SERVO CONTROL FOR THE ROTATIONAL SPEED

In this section we perform input-output linearization and design an LQ-servo controller to the (input-output) linearized model. Since the load torque (the third element of the disturbance vector d) cannot be measured directly, an appropriate estimator is constructed for this quantity. The linearization is done in two steps: the first step is a standard input-output linearization using the nominal model parameters, while the estimation of the load torque is solved in the second adaptive linearization step. The controlled plant is expected to follow a prescribed reference signal for the rotational speed.

4.1. Input-output linearization of the model with nominal load torque

The linearizing feedback can be written in the following standard form

$$u = \alpha(x) + \beta(x)w$$

where $\alpha, \beta \in \mathbb{R}^3 \mapsto \mathbb{R}$, and w is the new external input.

It is clear from (13) that the linearizing feedback is the following

$$\alpha(x) = -\frac{L_f^2 h_{ZD}(x)}{L_g L_f h_{ZD}(x)} \tag{14}$$

$$\beta(x) = \frac{1}{L_g L_f h_{ZD}(x)} \tag{15}$$

Let us use the following notations

$$\bar{z_1} = x_3 - x_3^* \tag{16}$$

$$\bar{z_2} = \dot{x}_3 \tag{17}$$

$$\bar{w} = w - w^* \tag{18}$$

where w^* is the necessary constant input value corresponding to the steady state x_3^*. Using (16)-(18) the linearized system model can be written as a simple double integrator:

$$\begin{bmatrix} \dot{\bar{z_1}} \\ \dot{\bar{z_2}} \end{bmatrix} = \begin{bmatrix} 0 & 1 \\ 0 & 0 \end{bmatrix} \begin{bmatrix} \bar{z_1} \\ \bar{z_2} \end{bmatrix} + \begin{bmatrix} 0 \\ 1 \end{bmatrix} \bar{w} \tag{19}$$

while the zero dynamics is given by

$$\dot{x_2} = \Phi(z_1, z_2, x_2), \tag{20}$$

where $\Phi(0,0,x_2) = \phi(x_2)$.

Since the input-output linearizing feedback is a state feedback, the state variables of the system have to be determined from the measured output variables. We assume that the state variables x_2 and x_3 are

measurable directly, while x_1 can be determined from the function h_1 in (11) using the measured value of d_1:

$$x_1 = \frac{V_{Comb}}{R}\frac{x_2}{y_1}\left(1-\eta_T\left(1-\left(\frac{d_1}{\sigma_I\sigma_N x_2}\right)^{\frac{\kappa-1}{\kappa}}\right)\right)$$

4.2. Input-output linearization with load torque estimation

Until now in was assumed that the external disturbances are known exactly. The first two elements of the disturbance vector ($d_1 = p_1^{tot}$ and $d_2 = T_1^{tot}$) are assumed to be measurable and constant, so the only difficulty is with the computation of the load torque ($d_3 = M_{load}$). This problem is solved by designing an adaptive control law that uses the estimation of d_3.

Let us denote the nominal value of d_3 by d_3^{nom}. Then the load torque can be rewritten as:

$$d_3 = d_3^{nom} + \mu$$

where μ is the deviance of d_3 from its nominal value. Assume now that d_3 (and therefore μ) is a constant. Using the fact that M_{load} appears additively in (3), we can write the derivative of y_{ZD} as

$$\dot{y}_{ZD} = \dot{x}_3 = f_3(x, d_3^{nom}) + l_1\mu$$

where

$$l_1 = -\frac{1}{2\pi\Theta}\frac{3}{50}$$

and

$$\begin{aligned} f_3(x, d_3^{nom}) &= \frac{1}{4\Pi^2\Theta n}\left(\nu_T c_p \frac{p_3^{tot}V_{Comb}}{m_{Comb}R}\eta_T\eta_{mech}\left(1-\left(\frac{p_1^{tot}}{p_3^{tot}\sigma_I\sigma_N}\right)^{\frac{\kappa-1}{\kappa}}\right)\right. \\ &- \left.\nu_C c_p \frac{T_1^{tot}}{\eta_C}\left(\left(\frac{p_3^{tot}}{p_1^{tot}\sigma_{Comb}}\right)^{\frac{\kappa-1}{\kappa}}-1\right) - 2\Pi\frac{3}{50}nd_3^{nom}\right) \end{aligned}$$

with the algebraic constraints (4)-(5) and the definition of x in (8). The second time-derivative of y_{ZD} is:

$$\ddot{y}_{ZD} = \sum_{i=1}^{3}\frac{\partial f_3(x,d)+l_1\mu}{\partial x_i}\Big(f_i(x,d)+g_i(x)u\Big) + + \frac{\partial f_3(x,d)+l_1\mu}{\partial x_3}l_1\mu + l_1\dot{\mu}$$

where f_i are the coordinate functions of f defined in (11). Using that μ is a constant, this equation becomes

$$\ddot{y}_{ZD} = \sum_{i=1}^{3} \frac{\partial f_3(x,d)}{\partial x_i} \Big(f_i(x,d) + g_i(x)u \Big) + \frac{\partial f_3(x,d)}{\partial x_3} l_1 \mu = L_f^2 h_{ZD}(x) + L_g L_f h_{ZD}(x)u + \psi(x,d^{nom})\mu$$

where $\psi(x,d^{nom}) = l_1 \frac{\partial f_3(x,d^{nom})}{\partial x_3}$, and d^{nom} denotes the disturbance vector with nominal disturbance values. Applying the feedback (14)-(15) and using the notations in (16)-(18) the system model becomes

$$\dot{\bar{z}}_1 = \bar{z}_2 \tag{21}$$

$$\dot{\bar{z}}_2 = \psi(x,d^{nom})\mu + \overline{w} \tag{22}$$

Comparing this model to the model (19), the only difference is the nonlinear term in the second differential equation. To cancel the effect of this nonlinearity, an adaptive controller is designed that estimates the value of μ.

Observe that the model (21)-(22) is in the following linearly parameterised input affine form:

$$\dot{\bar{z}} = \widetilde{f}(\bar{z}) + \widetilde{q}(x,d^{nom})\mu + \widetilde{g}(\bar{z})\overline{w}$$

where

$$\widetilde{f}(\bar{z}) = \begin{bmatrix} \bar{z}_2 \\ 0 \end{bmatrix}, \quad \widetilde{g}(\bar{z}) = \begin{bmatrix} 0 \\ 1 \end{bmatrix}, \quad \widetilde{q}(x,d^{nom}) = \begin{bmatrix} 0 \\ \psi(x,d^{nom}) \end{bmatrix}.$$

Let us apply to our model the so-called "Adaptive Feedback Linearization Theorem" [12] which will serve as a theoretical basis for the controller design.

Theorem 1.: Assume that for system (21)-(22)

(i) the nominal system is globally feedback linearizable,

(ii) the strict triangularity conditions $ad_{\widetilde{q}} G_i \subset G_i, \ 0 \le i \le \widetilde{n}-2$, (where $G_i = span\{\widetilde{g}, ad_{\widetilde{f}}^i \widetilde{g}\}$) are satisfied;

then there exists an adaptive feedback linearizing control.

It is important to note that the theorem above will be applied to the model (21)-(22) instead of the open loop turbine model. Its is easy to see that the feedback linearization of the model (21)-(22) is equivalent to the input-output linearization of the model defined by (21)-(22) and the additional zero dynamics (20). Also note that although the feedback that will be computed feedback linearizes (21)-(22) **globally**, this feedback will only be applied to the turbine model inside its operating domain $\mathscr{X}$.

Since the nominal system (i.e. (21)-(22) with $\mu = 0$) is globally feedback linearizable with $\bar{w} = 0$, the first condition is satisfied. Furthermore, the dimension of the model (21)-(22) is $\tilde{n} = 2$, which means that only $ad_{\tilde{q}}G_0 \subset G_0$ has to be checked, where $G_0 = span\{\tilde{g}\}$:

$$ad_{\tilde{q}}G_0 = \frac{\partial \tilde{g}}{\partial \bar{z}}\tilde{q} - \frac{\partial \tilde{q}}{\partial \bar{z}}\tilde{g} = -\begin{bmatrix} 0 & 0 \\ \frac{\partial \psi}{\partial \bar{z}_1} & \frac{\partial \psi}{\partial \bar{z}_2} \end{bmatrix}\begin{bmatrix} 0 \\ 1 \end{bmatrix} = \begin{bmatrix} 0 \\ -\frac{\partial \psi}{\partial \bar{z}_2} \end{bmatrix} \subset span\left\{\begin{bmatrix} 0 \\ 1 \end{bmatrix}\right\} = G_0$$

Since both conditions are satisfied, the adaptive feedback linearizing control can be computed in the following way (see pages 119-120. in [12]). Define a reference model

$$\begin{bmatrix} \dot{\bar{z}}_{r1} \\ \dot{\bar{z}}_{r2} \end{bmatrix} = A_r \begin{bmatrix} \bar{z}_{r1} \\ \bar{z}_{r2} \end{bmatrix} + \begin{bmatrix} 0 \\ 1 \end{bmatrix} w_r \quad , \quad A_r = \begin{bmatrix} 0 & 1 \\ -k_1 & -k_2 \end{bmatrix}$$

where $s^2 + k_2 s + k_1$ is a Hurwitz polynomial (i.e. A_r is a stability matrix). Denote the estimated value of μ by $\hat{\mu}$ and the estimation error by $\Delta\mu$:

$$\Delta\mu = \mu - \hat{\mu} \tag{23}$$

Define the following control input function:

$$\bar{w} = -\psi(x, d^{nom})\hat{\mu} - k_1\bar{z}_1 - k_2\bar{z}_2 + w_r \tag{24}$$

where w_r is the common input variable of both the controlled system model and the reference model,

and substitute it to the model (21)-(22):

$$\dot{\bar{z}}_1 = \bar{z}_2 \tag{25}$$

$$\dot{\bar{z}}_2 = -k_1\bar{z}_1 - k_2\bar{z}_2 + \psi(x, d^{nom})\Delta\mu + w_r \tag{26}$$

Define the reference error e as

$$e = \begin{bmatrix} e_1 \\ e_2 \end{bmatrix} = \begin{bmatrix} \bar{z}_1 \\ \bar{z}_2 \end{bmatrix} - \begin{bmatrix} \bar{z}_{r1} \\ \bar{z}_{r2} \end{bmatrix}$$

Then the reference error dynamics reads

$$\begin{bmatrix} \dot{e}_1 \\ \dot{e}_2 \end{bmatrix} = A_r \begin{bmatrix} e_1 \\ e_2 \end{bmatrix} + \begin{bmatrix} 0 \\ \psi(x, d^{nom}) \end{bmatrix} \Delta\mu$$

where the dynamics of μ is not determined yet. Let P be the positive definite solution of the Lyapunov equation

$$A_r^T P + PA_r = -I$$

where $I \in \mathbb{R}^{2\times 2}$ is the identity matrix. Consider the following positive definite Lyapunov function candidate:

$$V = e^T Pe + \gamma\Delta\mu^2\,, \quad \gamma \in \mathbb{R}$$

The time derivative of V is given by

$$\frac{d}{dt}V = -e_1^2 - e_2^2 + 2\begin{bmatrix} e_1 & e_2 \end{bmatrix} P \begin{bmatrix} 0 \\ \psi(x, d^{nom}) \end{bmatrix} \Delta\mu + \frac{2}{\gamma}\Delta\mu\frac{d}{dt}\Delta\mu$$

By choosing the following adaptation error dynamics

$$\frac{d}{dt}\Delta\mu = -\gamma\begin{bmatrix} e_1 & e_2 \end{bmatrix} P \begin{bmatrix} 0 \\ \psi(x, d^{nom}) \end{bmatrix},$$

the time derivative becomes

$$\dot{V} = -e_1^2 - e_2^2$$

which is negative definite, therefore V is a Lyapunov function and the adaptation error asymptotically converges to zero.

Differentiating (23) by time and using that μ is a constant, the adaptation law can be determined from the adaptation error dynamics:

$$\frac{d}{dt}\widehat{\mu} = \gamma \begin{bmatrix} e_1 & e_2 \end{bmatrix} P \begin{bmatrix} 0 \\ \psi(x, d^{nom}) \end{bmatrix} = -\frac{d}{dt}\Delta\mu \tag{27}$$

Thus, the controller designed to (21)-(22) with the control input (24) and adaptation law (27) successfully performs adaptive feedback linearization and stabilisation of (21)-(22), moreover, it gives an (asymptotically converging) estimate $\widehat{\mu}$ of the unknown parameter μ.

4.3. Servo controller with stabilising feedback

Our aim is to build a controller that tracks the reference signal y_{3ref} that is our prescribed value for the rotational speed. For this purpose, an LQ-servo controller is designed.

Observe that in the control input defined in (24), the parameters k_1 and k_2 have not been determined yet. These parameters can be computed as the result of a simple LQ design to the double integrator model (19). Additionally, by choosing $w_r = k_1 y_{3ref}$, the controlled plant will track a prescribed piecewise constant reference signal. Since $\lim_{t\to\infty}\Delta\mu = 0$, the only steady state operating point of (25)-(26) is $\bar{z}_1 = y_{ref}$, $\bar{z}_2 = 0$ which is unique, and - because of the LQ controller - it is asymptotically stable.

The tuning parameters of the controller are the positive definite state and input weighting matrices ($Q \in \mathbb{R}^{2\times 2}$ and $R \in \mathbb{R}^{1\times 1}$, respectively), and the adaptation coefficient γ in (27). Let $R = 1$ be fixed. For the sake of simplicity, the Q is restircted to be diagonal: $Q = diag(Q_{11}, Q_{22})$.

Now, three scalar parameters (Q_{11}, Q_{22} and γ) are to be determined according to the following control goals:

1. let the settling time of the rotational speed between 1.5 s and 2 s;
2. let the plant be robust against uncerainties in environmental disturbances and model parameters;
3. avoid the saturation of the actuator (the control input u is bounded: $0 \leq u \leq 0.03\ kg/s$)

The tuning of parameters is successfully performed via simulations in Matlab/Simulink using piecewise constant reference signals (for Goal 1) and 'worst case' disturbances/uncertainties (for Goals 2 and 3). The resulted design parameters are:

$$Q = \begin{bmatrix} 3 \times 10^5 & 0 \\ 0 & 1.5 \times 10^5 \end{bmatrix}, \quad \gamma = 25$$

It is important to note that (according to [12]) time-varying parameters are also allowed, if they can be modelled by the following exosystem with unknown initial condition μ_0:

$$\dot{\mu} = \Omega(t,x)\mu + \omega(t,x) \tag{28}$$

if $\Omega^T + \Omega$ is negative semidefinite, when $t \geq 0$, and the exosystem is bounded input (x) bounded state (μ). During simulations, only such μ functions will be used that can be modeled with $\Omega = 0$.

5. SIMULATION RESULTS

The simulations were performed using the Matlab/Simulink software environment. For the integration of the model equations, the built-in 'ode45' ordinary differential equation solver was applied, which is based on a Runge-Kutta (4,5) formula [13].

In Fig. 3, the subfigures show the time function of the control input and of the rotational speed - v_{fuel} and n respectively -, near typical values of parameters and environmental disturbances. The load torque is set to its nominal value: $M_{load} = 50\ Nm$. The rotational speed (solid line in the second subfigure) is started from $n = 750\ \frac{1}{s}$ and tracks a piecewise constant reference signal (dashed line in

the second subfigure). The settling time of the transient is about $t_s = 1.7\ s$. The related control input function is depicted in the first subfigure. This simulation demonstrates that the controlled nominal plant is asymptotically stable and tracks the reference signal with linear transients.

The operation of the adaptive controller is shown in Fig. 4. The second subfigure shows the estimation of the load torque. The time function of the load torque (dashed line) consists of linear and constant pieces, that are followed well by the estimated value (solid line). The estimation contains some little drops/overshoots at time instances $2, 4, 5.5, 7\ s$ caused by the fast changes in the load torque function. The third subfigure shows the reference tracking for the rotational speed with the same reference signal as in Fig. 3. This reference signal is successfully tracked, and large changes in the load torque cause only transients of small magnitude in the rotational speed. The first subfigure shows the related control input function. It is important to mention that the drops/overshoots in the estimation of the load torque does not affect the rotational speed or the control input significantly.

5.1. Robustness

To test the proposed control scheme under more realistic circumstances, we now relax the original assumptions that all the model parameters and disturbances (with the exception of the load torque) are known.

Figure 5 demonstrates the 'worst case' behaviour of the plant against model parameter uncertainties and environmental disturbances: This simulation shows the reference tracking when three model parameters having a significant effect on the dynamical behaviour are uniformly set to their maximal/minimal/nominal values together with p_1 and T_1. The applied minimal and maximal

parameter and disturbance values were the following:

$$\min V_{Comb} = 0.0053m^3 \quad , \quad \max V_{Comb} = 0.0061m^3$$

$$\min \Theta = 0.0003kgm^2 \quad , \quad \max \Theta = 0.0005kgm^2$$

$$\min \eta_{comb} = 0.74768 \quad , \quad \max \eta_{comb} = 0.82048$$

$$\min p_1^{tot} = 90000Pa \quad , \quad \max p_1^{tot} = 110000Pa$$

$$\min T_1^{tot} = 268.15K \quad , \quad \max T_1^{tot} = 303.15K$$

$$\min M_{load} = 0Nm \quad , \quad \max M_{load} = 150Nm$$

The load torque (second subfigure) - was simultaneously set to its minimal and maximal value (0 Nm and 150 Nm, respectively).

The prescribed rotational speed trajectory (dashdot line in the third subfigure) differs from the former ones in order to show not just the transient, but also the steady state behaviour (between 3 s and 6.5 s) of the plant in a more realistic environment.

The trajectories of the rotational speed corresponding to the maximal/ minimal/ nominal values of uncertain model parameters are denoted by solid/dashed/dotted lines, respectively in the third subfigure. The same line styles are used for the related control input functions in the first subfigure. The effect of model parameter uncertainties can be observed in the beginning of the time function of the rotational speed, showing that the LQ-servo controller successfully suppresses their influence: the rotational speed trajectories overlap (third subfigure), the only slight difference is between the related control input functions (first subfigure). Although the changes of the load torque (as external disturbance) are non-smooth with the possible largest magnitude, they cause only tiny drops/overshoots in the time function of the rotational speed, which converges back to the prescribed reference value in a very short time.

It is also visible that the control input is far from saturation since it is between $5 \times 10^{-3} \frac{kg}{s}$ and $17 \times 10^{-3} \frac{kg}{s}$, while the saturation bounds are $0 \frac{kg}{s}$ and $30 \times 10^{-3} \frac{kg}{s}$.

Another case study is performed and illustrated in Fig. 6 in order to show the effect of environmental disturbances not just on reference tracking, but also on the adaptive estimation of the load torque. Four different simulations are reported here: with minimal p_1^{tot} and T_1^{tot} values (denoted by dotted line), with minimal p_1^{tot} and maximal T_1^{tot}, and with maximal p_1^{tot} and minimal T_1^{tot} values (both denoted by dashed lines), and with maximal p_1^{tot} and T_1^{tot} values (denoted by solid line). The only significant difference is between the control input functions (first subfigure).

The time-function of the load torque consists of linear and constant pieces (dash-dot line in the second subfigure. Large drops/overshoots in the estimation of the load torque only occur between 1 *s* and 8 *s*, caused by the quick changes in the load torque. It is also shown that there is no significant difference between the estimations of the load torque belonging to different extrema of p_1^{tot} and T_1^{tot} (these four curves overlap).

The reference signal for the rotational speed (dash-dot line in the third subfigure) is a staircase-like piecewise constant function which is successfully tracked. The little drops/overshoots between 1 *s* and 8 *s* are caused by the sudden changes of the highest magnitude in the time function of the load torque. The time functions of the rotational speed belonging to different extrema of p_1^{tot} and T_1^{tot} overlap during the whole simulation. Note that the control input is far from saturation just like in the former simulation studies.

6. CONCLUSIONS

In this paper, a nonlinear model of a low-power gas turbine has been built from first engineering principles which is suitable for control purposes. Because of the algebraic complexity of the

one-dimensional zero dynamics model of the turbine with the rotational speed held constant, the stability neighbourhood of its operating points were estimated with phase diagrams and found to be asymptotically stable in all examined cases. An adaptive input-output linearizing and LQ-servo control loop has been built to track a given piecewise constant reference signal for the rotational speed. The adaptive control scheme includes the estimation of the load torque which is an important time-varying parameter in the system. Simulations showed that the controlled plant fulfills the required performance criteria, and the reference tracking is sufficiently robust against both environmental disturbances and model parameter uncertainties. Moreover, the result of the torque estimation is accurate and well usable even when the environmental parameters change in the examined range.

ACKNOWLEDGEMENTS

This work has been supported by the Hungarian National Research Fund through grants no. $K67625$ and $F046223$ which are gratefully acknowledged. The fourth author is the grantee of the Bolyai János Scholarship of the Hungarian Academy of Sciences.

REFERENCES

1. Evans C. Testing and modelling aircraft gas turbines: Introduction and overview. *Prep. UKACC International Conference on Control'98* 1998.
2. Perez RA. Model reference control of a gas turbine engine. In *Proceedings of the Institution of Mechanical Engineers - Part G: Journal of Aerospace Engineering* 1996; **210**:291–296.
3. Athans M, Kapasouros P, Kappos E, Spang HA. Linear-quadratic gaussian with loop-transfer recovery methodology for the F-100 engine. *IEEE Journal of Guidance and Control* 1986; **9**(1):45–52.
4. Ariffin AE, Munro N. Robust contol analysis of a gas-turbine aeroengine. *IEEE Transactions on Control Systems Technology* 1997; **5**(2):178–188.
5. Kulikov GG, Thompson HA. *Dynamic Modelling of Gas Turbines: Identification, Simulation, Condition Monitoring and Optimal Control.* Springer, 2004.

6. Marino R, Tomei P, Verrelli CM. Adaptive control for speed-sensorless induction motors with uncertain load torque and rotor resistance. *International Journal of Adaptive Control and Signal Processing* 2005; **19**(9):661-685. DOI: 10.1002/acs.874
7. Tang X, Tao G, Joshi SM. Adaptive output feedback actuator failure compensation for a class of non-linear systems. *International Journal of Adaptive Control and Signal Processing* 2005; **19**(6):419-444. DOI: 10.1002/acs.843
8. Ailer P, Sánta I, Szederkényi G, Hangos KM. Nonlinear model-building of a low-power gas turbine. *Periodica Polytechnica Ser. Transportation Engineering* 2001; **29**(1-2):117–135.
9. Ailer P, Szederkényi G, Hangos KM. Model-based nonlinear control of a low-power gas turbine. In *Proceedings of the 15th IFAC World Congress on Automatic Control*, Camacho EF, Basanez L, de la Puente JA (eds). Elsevier Science, 2002.
10. Isidori A. *Nonlinear Control Systems*. Springer, 1995.
11. Ailer P, Szederkényi G, and Hangos KM. Parameter-estimation and model validation of a low-power gas turbine. In *Proceedings of the "Modelling, Identification and Control'2002" Conference*, Hamza MH (eds). ACTA Press, 2002; 604–609,
12. Marino R, Tomei P. *Nonlinear Control Design: Geometric, Adaptive, and Robust*. Prentice Hall, 1995.
13. Dormand JR, Prince PJ. A family of embedded Runge-Kutta formulae. *Journal of Computational and Applied Mathematics* 1980; **6**:19–26.
14. Chipperfield AJ, Bica B, Fleming PJ. Fuzzy scheduling control of a gas turbine aero-engine: a multiobjective approach. *IEEE Tr. on Industrial Electronics* 2005; **49**:536–548.
15. Kurd Z, Kelly, TP. Using safety critical artificial neural networks in gas turbine aero-engine control. *Lecture Notes in Computer Science* 2005; **3688**:136–150.
16. Lin ST, Yeh LW. Intelligent control of the F-100 turbofan engine for full flight envelope operation. *International Journal of Turbo & Jet-Engines* 2005; **22**:201–213.
17. Jurado F, Carpio J. Improving distribution system stability by predictive control of gas turbines. *Energy Conversion and Management* 2006; **47**:2961–2973.
18. Mu J, Rees D, Liu GP. Advanced controller design for aircraft gas turbine engines. *Control Engineering Practice* 2004; **13**:1001–1015.
19. Brunell BJ, Bitmead RR, Connolly AJ. Nonlinear model predictive control of an aircraft gas turbine engine. *Proc. of the 41st IEEE Conference on Decision and Control, Las Vegas, Nevada USA* 2002.
20. Zweiri YH, D Seneviratne L. Diesel engine indicated and load torque estimation using a non-linear observer. *Proc. of the Institution of Mechanical Engineers Part D - Journal of Automobile Engineering* 2006; **220**:775–785.
21. Goedtel A, da Silva IN, Serni PJA. Load torque identification in induction motor using neural networks technique. *Electric*

Power Systems Research 2007; **77**:35–45.

NOMENCLATURE OF THE TURBINE MODEL

	Variables/Constants
A	area $[m^2]$
E	mechanical energy $[J]$
M	torque $[Nm]$
Q_f	lower thermal value of fuel $[J/kg]$
R	specific gas constant $[J/(kgK)]$
T	temperature $[K]$
U	internal energy $[J]$
V	volume $[m^3]$
a_1, a_2	coefficients of q_1 $[s]$
a_3, a_4	coefficients of q_1 $[-]$
$b_i,\ i = 1,..,4$	coefficients of q_3 $[-]$
c	specific heat $[J/(kg\,K)]$
m	mass $[kg]$
n	rotational speed $[1/s]$
p	pressure $[Pa]$
t	time $[s]$
β	specific par. of air & gas $[\sqrt{K}s/m]$
η	efficiency $[-]$
θ	inertial moment $[kg\,m^2]$
κ	adiabatic exponent $[-]$
ν	mass flowrate $[kg/s]$
σ	pressure loss coefficient $[-]$
τ	turbine velocity coefficient $[\sqrt{K}s]$

	Subscripts
0	inlet duct inlet
1	compressor inlet
2	compressor outlet
3	turbine inlet
4	turbine outlet
C	refers to compressor
$Comb$	refers to combustion chamber
$comb$	refers to combustion
$fuel$	refers to fuel
I	refers to inlet duct
$load$	load
$mech$	mechanical
N	refers to gas deflector
p	refers to constant pressure
$schaft$	refers to schaft
T	refers to turbine
v	refers to constant volume

	Superscripts
tot	refers to a total quantity

FIGURES

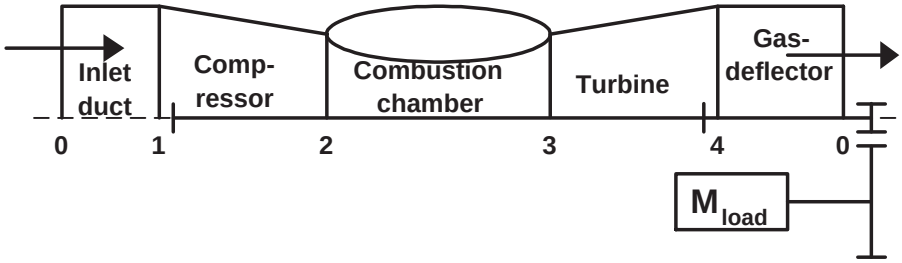

Figure 1. The main parts of the gas turbine

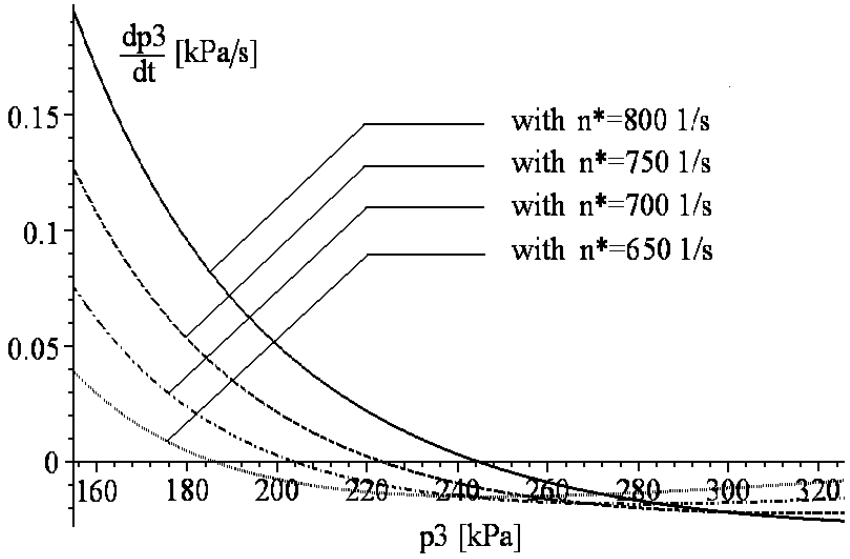

Figure 2. Phase diagram for the system with four constant rotational speed values

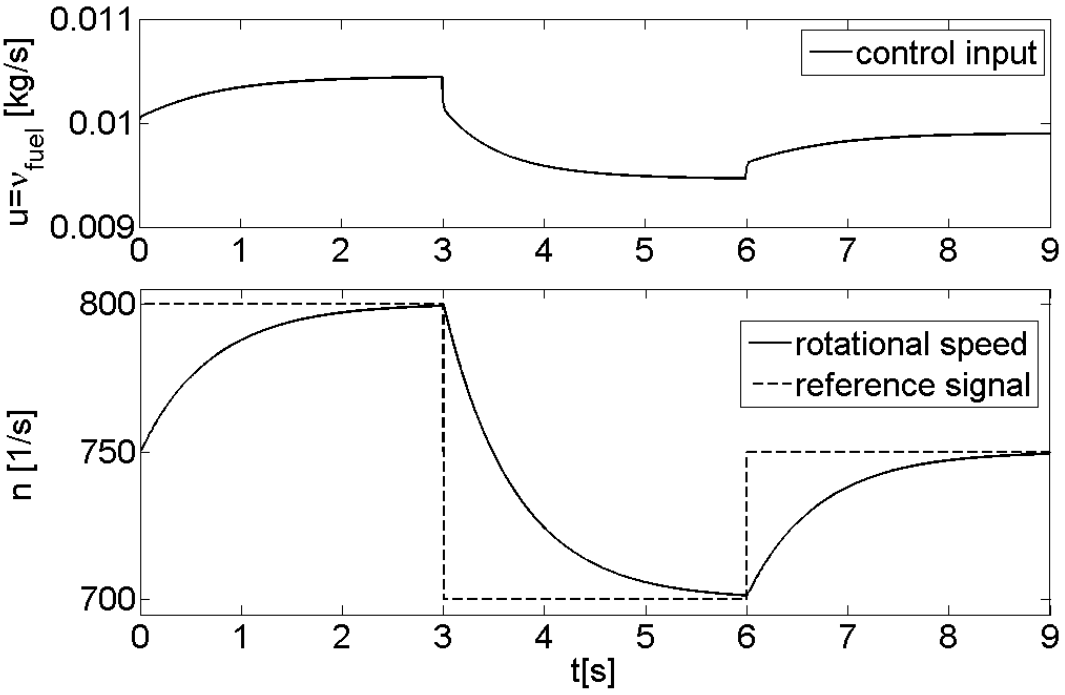

Figure 3. Reference signal tracking for the rotational speed

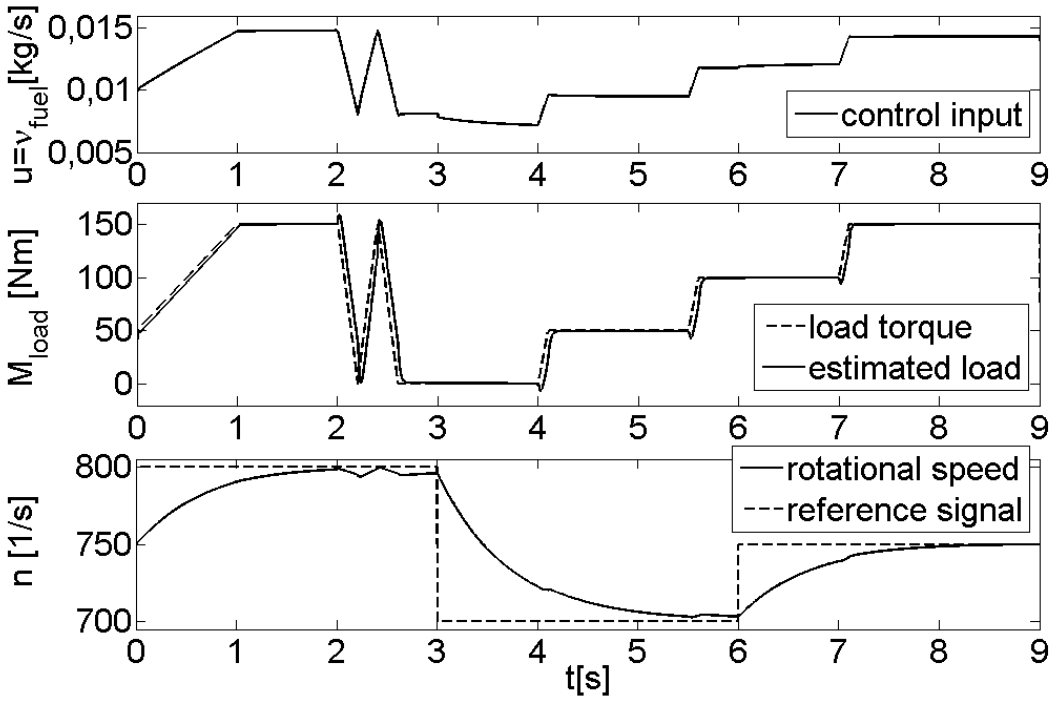

Figure 4. Estimation of the load torque

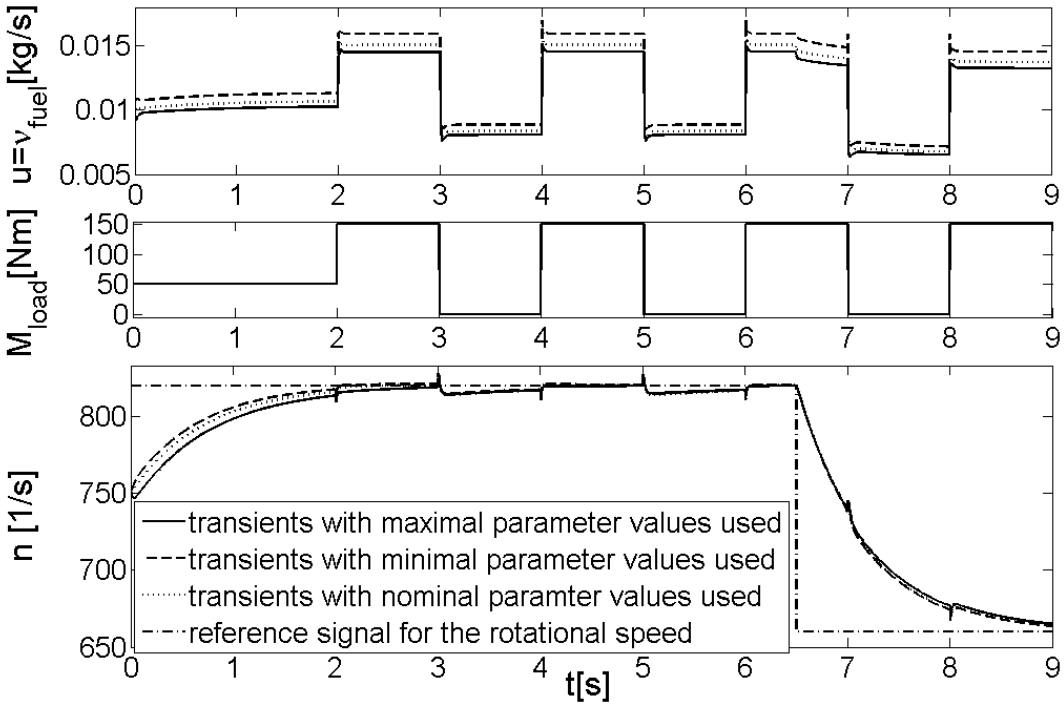

Figure 5. Robustness of the proposed control scheme I.(curves overlap in subfigures 2 and 3)

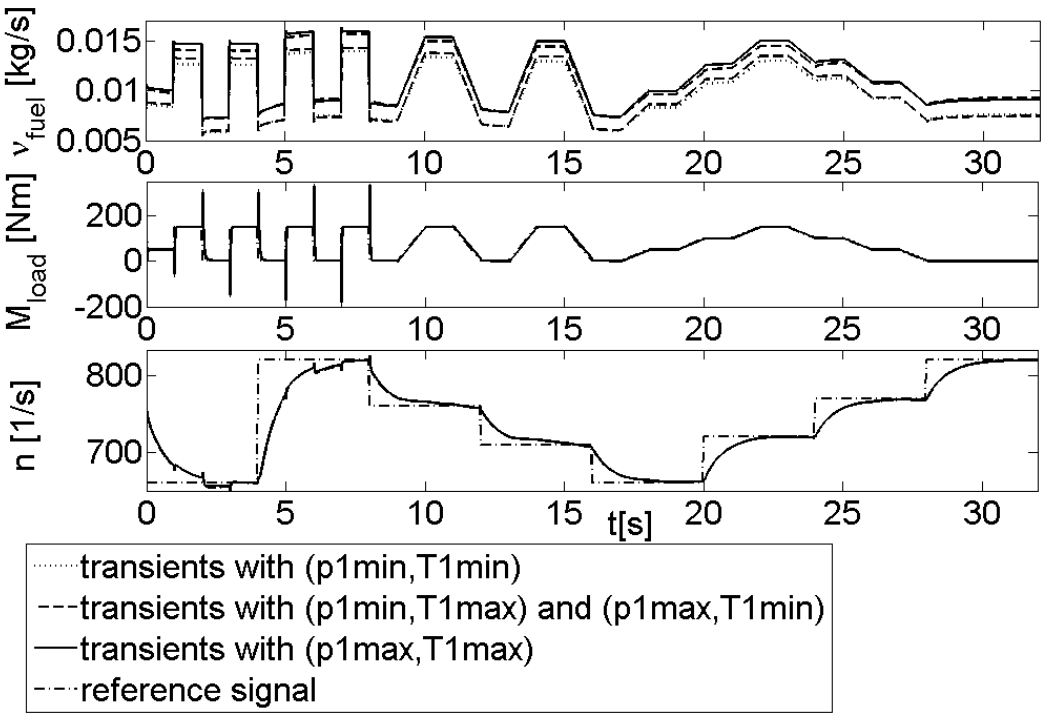

Figure 6. Robustness of the proposed control scheme II. (curves overlap in subfigures 2 and 3)

TABLES

Table I. State, input, output and disturbance variables (see the Nomenclature for further details)

Notation	**Variable name/Units**	**Notation**	**Variable name/Units**
m_{Comb}	mass in combustion chamber $[kg]$	p_1^{tot}	compressor inlet total pressure $[Pa]$
p_3^{tot}	turbine total inlet pressure $[Pa]$	T_1^{tot}	compressor inlet total temperature $[K]$
n	rotational speed $[1/s]$	M_{load}	load torque $[Nm]$
v_{fuel}	mass flowrate of fuel $[kg/s]$	T_4^{tot}	turbine outlet total temperature $[K]$

APPENDIX

Table II. Constants of the simplified model of the DEUTZ T216 type turbine

Not.	**Value**	**Not.**	**Value**
R	287 $J/(kg\,K)$	β	0.0404184 $\sqrt{K}s/m$
c_p	1004.5 $J/(kg\,K)$	c_v	717.5 $J/(kg\,K)$
κ	1.4	τ	0.028071 $\sqrt{K}s$
Q_f	42.8 MJ/kg	T_0	288.15 K
A_1	0.0058687 m^2	A_3	0.0117056 m^2
σ_N	0.96687	σ_I	0.98879
σ_{Comb}	0.93739		
η_C	0.67585	η_T	0.85677
η_{comb}	0.79161	η_{mech}	0.9801
Θ	0.0004 $kg\,m^2$	V_{Comb}	0.005675 m^3
a_1	0.00035319 s	a_2	0.0011097 s
a_3	-0.4611	a_4	0.16635
b_1	-0.033728	b_2	0.004458
b_3	0.048847	b_4	0.15542